Evolution & Development

WILEY

RESEARCH ARTICLE

Endosymbiont Interactions With the Germline Underlie a Case of Evolutionary Novelty in Carpenter Ants

Zelal Özgür Durmuş[1,2] | Nihan Sultan Milat[2,3] | Arjuna Rajakumar[4] | Ab. Matteen Rafiqi[2]

[1]Graduate School of Science and Engineering, Hacettepe University, Ankara, Turkiye | [2]Beykoz Institute of Life Sciences and Biotechnology, Bezmialem Vakif University, Istanbul, Turkiye | [3]Institute of Health Sciences, Bezmialem Vakif University, Istanbul, Turkiye | [4]Whitehead Institute, Cambridge, Massachusetts, USA

Correspondence: Ab. Matteen Rafiqi (m.rafiqi@bezmialem.edu.tr)

Received: 16 April 2025 | **Revised:** 17 October 2025 | **Accepted:** 20 November 2025

Keywords: cell fusion | developmental plasticity | endosymbiosis | evolutionary novelty | germline

ABSTRACT

Evolutionary novelties often arise through complex interactions among genetic, developmental, and ecological processes, yet their origins remain poorly understood. Here, we investigate the germline capsule in *Camponotus* (Carpenter ants) as a case of an evolutionary novelty. Using an integrated framework combining transcriptomic, morphological, and comparative developmental approaches, we characterize its molecular signatures, cellular architecture, and ontogeny. We show that germline gene–expressing cells adjacent to bacteriocytes fuse to form a multinucleated germline capsule, which subsequently contributes to the presumptive gonads, as revealed by label tracing. Despite harboring endosymbiotic bacteria like bacteriocytes, germline capsules exhibit distinct gene expression profiles. Furthermore, their phenotypic variation is developmentally modulated by bacterial presence. By examining the expression profile of germ-line specific gene (*oskar*) across multiple *Camponotus* species, we test the germline function of the capsule and its evolutionary conservation. Based on these findings, we propose a model in which the germline capsule evolved through cell fusion events enabled by developmental plasticity and shaped by interactions between host germline determinants and endosymbiotic bacteria. This study illustrates how integrating molecular, developmental, and ecological perspectives can illuminate the mechanisms underlying evolutionary innovation.

1 | Introduction

An evolutionary novelty is a new trait, or a novel combination of previously existing traits, that arises during the evolution of a lineage and may result in a new long-lasting consequence for that lineage (Pigliucci 2008). A novelty should represent qualitative shifts in form or function that can open up new adaptive possibilities or more niche opportunities (Erwin 2021; Müller and Newman 2005). However, the emergence of a new trait does not always mean that it will become stable within a lineage or lead to changes at macro-level; it often requires integration with other traits and refinement through developmental and ecological interactions (Galis 2001; Wagner 2014). The mechanisms for the origin and subsequent persistence of a novelty at the genetic level -such as gene duplication and regulatory network evolution- have been studied extensively over the past several decades (Davidson and Erwin 2006; Garcia-Fernàndez and Holland 1994; Wray 2007; Zhang 2003). It is being increasingly recognized that alterations in developmental pathways, developmental plasticity, and the influence of developmental endosymbionts working at multi-levels of biological organization contribute to trait diversity (Abouheif et al. 2014; Gilbert et al. 2015; Moczek et al. 2011; West-Eberhard 2005).

In organisms with intracellular endosymbionts, developmental endosymbiosis—the integration of these symbionts into host developmental processes—has recently been recognized to influence host traits (Gilbert et al. 2015; McFall-Ngai et al. 2013;

Summary

- In the carpenter ants, a novel cell type called the germline capsule, representing a unique cellular compartment distinct from other known cell types of this lineage, has been identified. We study this structure as a case of possible evolutionary novelty.
- The germline capsule likely plays a specialized function in the vertical transmission of the germline.
- Transcriptomic profiling reveals that the germline capsule has a distinct transcriptional signature, characterized by upregulation of autophagy-related genes and endomembrane components, and downregulation of translational and ribosomal activity.
- The germline capsule exhibits developmental plasticity and sensitivity to the bacterial microenvironment in *Camponotus floridanus*, and its phenotype varies across species within the *Camponotus* genus.
- Potential co-expression of germline genes *oskar* and *vasa*, along with low bacterial load, facilitates the fusion of bacteriocyte-bordering germline cells, leading to the evolution of the germline capsule.

Rafiqi et al. 2022). However, how endosymbiont influences the emergence of evolutionary novelties has rarely been described (Montgomery and McFall-Ngai 1994). Endosymbiosis involves the intimate and sustained interaction between the partners, often beginning early in development and continuing throughout the life cycle. The endosymbiotic partner acts as a microenvironmental factor that induces different phenotypic outcomes in a given host genotype, thereby making developmental endosymbiosis a distinct form of development. How processes such as developmental endosymbiosis contribute to the evolution of novelty remains an open question.

In the carpenter ant, *Camponotus floridanus* (*C. floridanus*), endosymbiotic bacteria *Blochmannia* have resulted in significant alterations in embryonic development (Rafiqi et al. 2020). These alterations include potentially novel characters in at least two cell types both of which carry the endosymbiont; the bacteriocytes, and a large multi-nucleated cell called "germline capsule." A majority of the endosymbionts are housed in the bacteriocytes, which eventually become part of the midgut epithelium. A minority of the bacteria is housed in the germline capsule, which has been hypothesized to function in the vertical transmission of the endosymbiont in addition to being the functional germline (Rafiqi et al. 2020). The germline identity of the capsule is hinted by the presence of germ granules composed of mRNAs and proteins of germline genes, which together function to specify, maintain, and transport germ cells toward their ultimate fate in insects (Extavour and Akam 2003; Pamula and Lehmann 2024; Saffman and Lasko 1999; Santos and Lehmann 2004). Similar to other insects, ants establish their germline at the posterior pole of the egg (Khila and Abouheif 2008). In *C. floridanus* however, the germline gene *oskar*, which is necessary and sufficient for imparting germline idenitity in *D. melanogaster* (Ephrussi and Lehmann 1992), appears to mark two places; the germline capsule and the germline at the posterior pole. This structure has been described in five species out of eight studied so far in the *Camponotus* genus (Rafiqi et al. 2020). Together, these observations point to the germline capsule as a distinctive structural feature of *Camponotus* of which the developmental and functional significance remains to be explored.

Here, we investigate the process of development of the germline capsule. We examined differential gene expression to identify pathways that are upregulated or downregulated in the germline capsule relative to earlier embryonic stages and bacteriocytes. We also explored phenotypic variability of the germline capsule in *C. floridanus* and two other species within this genus. Based on our results, we present a hypothesis for the evolution of the germline capsule within the context of developmental endosymbiosis. Our study contributes to a growing body of work that recognizes endosymbiosis as a potent player in development and evolution. This will open the possibility to study the germline capsule as one of the tangible examples of evolutionary novelty.

2 | Materials and Methods

2.1 | Rearing of Ant Colonies and Collection of Eggs

C. floridanus, *Camponotus nicobarensis*, and *Camponotus auriventris* colonies were reared in plastic containers equipped with glass test tubes filled with water and sealed with cotton wool. Colonies were provided with a mixed diet consisting of the Bhatkar–Whitcomb food (Bhatkar and Whitcomb 1970), cockroaches, and a 50% honey-water solution (wt/wt). Environmental conditions were maintained at 25°C with 50% relative humidity and a 12-h light/dark cycle.

For egg collection, queens from separate colonies of each species were placed individually into identical setups, accompanied by 5–10 workers from the same colony. Eggs were collected the day after queen isolation. Embryos were collected for various downstream applications, including nuclear staining, hybridization chain reaction (HCR), immunostaining, and transcriptomic analysis. For nuclear staining, HCR, and immunostaining, embryos were harvested across a range of developmental stages to enable screening of morphological and molecular features at different time points.

2.2 | Stage Identification

The stages were identified according to criteria set down in (Rafiqi et al. 2020) and (Chen et al. 2025). Briefly, we refer to stage 1 as freshly laid eggs, and stage 2 as the stage when first two nuclear division have completed. After this stage, all syncytial stages were treated as early stages, before cellularization of the syncytium, which we infer to be before zygotic gene expression based on *Monomorium* and *Drosophila* (Rajakumar et al. 2024). Stage 4 is the presyncytium stage, identified as the stage when the nuclei are placed peripherally but completed cells are not observed. The blastoderm stage is identified as stage 5; at this stage, the cellularization of the syncytium is completed, resulting in a fully cellularized single layer of cells in

the periphery of the egg, and the germline capsule is seen ventrally at about 80% egg length taking anterior as 0%. Stage 6 is defined by the appearance of ventral mesoderm invagination, stage 7 as the elongation of the germdisc making the germband. Stage 8 is identified as the stage when the germband is extended so that it touches the bacteriocyte cell mass posteriorly, and the capsule is positioned in the posterior-most part of the egg. Stage 10 is identified as the stage when the germband covers the entire ventral side beneath the egg shell from the anterior pole to the posterior pole of the egg, and stage 15 is identified as the stage when dorsal closure is completed, and stage 16 is identified as the stage when the pre-larva obtains its final head-shape.

2.3 | Antibiotics Treatment

Two mature colonies were treated with rifampicin to test the effects of *Blochmannia* on the formation of the germline capsule of *C. floridanus*. Rifampicin powder (Sigma; R883) was dissolved in water at a stock concentration of 2 mg/ml and then diluted 1:1 in a 50% honey–water solution. Colonies were given fresh rifampicin–honey–water three times a week for 2 months. After 2 months, embryos were collected, fixed, and stained with DAPI (4′,6-diamidino-2-phenylindole; Sigma-Aldrich) as described below to confirm elimination of *Blochmannia*. Then, the bacteria-eliminated eggs were collected for morphological analysis.

2.4 | Embryo Fixation and Dissection

Embryos collected for nuclear staining, HCR, and immunostaining were fixed by using formaldehyde following established protocols (Khila and Abouheif 2009; Rafiqi et al. 2011). Before formaldehyde fixation, heat fixation was applied for nuclear staining and HCR by immersing embryos in boiling phosphate-buffered saline (PBS) with Triton (PBT: 1.86 mM NaH_2PO_4, 8.41 mM Na_2HPO_4, 1.75 M NaCl, 0.03% Triton-X-100, pH 7.4). Embryos were then transferred to a second fixation solution containing 400 µL PEM, 500 µL heptane, and 60 µL formaldehyde. For immunohistochemistry, embryos were fixed only in PEMS buffer (100 mM PIPES, 2 mM $MgSO_4$, 1 mM EGTA, pH 6.9) and digested with proteinase K (0.08 U/mL in PBS, Invitrogen). Following fixation, embryos were washed with ice-cold distilled water, then shaken in methanol to crack the membranes. Subsequently, the chorion and vitelline membrane were manually removed using fine forceps. Embryos destined for transcriptomic analysis were fixed by using only heat fixation. Capsule and bacteriocytes were gently dissected under RNase-free conditions, pooled in TRIzol, and frozen before RNA extraction.

2.5 | DAPI Staining, Hybridization Chain Reaction, and Immunohistochemistry

Following vitelline membrane removal, embryos were rehydrated through a graded methanol-to-PBTw series (75%, 50%, 25%) (PBS: 137 mM NaCl, 2.7 mM KCl, 10 mM Na_2HPO_4, 1.8 mM KH_2PO_4; pH 7.4 supplemented with 0.1% Tween-20) and then washed thoroughly in PBTw. After rehydration, embryos were incubated with DAPI diluted 1:1000 in PBTw for 30 min at room temperature in the dark. Embryos were then equilibrated in a graded glycerol/PBS series (25%, 50%, 75%) and mounted in 75% glycerol in PBS for imaging. DAPI staining was performed to visualize host cell nuclei and assess nuclear positioning, organization throughout early embryogenesis in the germline capsule, focusing on stages 5 to 8 when this novel cell type emerges and becomes distinct. In addition, we stained embryos from multiple colonies and observed differences in the morphology of the germline capsule in later stages. We mainly focused on the subcellular structural features in the embryo with microscopic detail, especially between stages 5 and 8. We used confocal microscopy to track host nuclei, the bacteria, and the general structure of the embryo in relation to the germline capsule.

For HCR, embryos were fixed as described above. The reaction was performed using standard protocols provided by Molecular Instruments (Choi et al. 2018). A total of 20 probe pairs were designed against *C. floridanus oskar* (LOC105249250) and synthesized by the manufacturer. HCR was used to detect the spatial expression of *oskar*, a conserved germ granule component and germline marker. This allowed us to localize *oskar* transcripts within developing embryos, particularly within the germline capsule and neighboring cells, to assess germline specification and spatial compartmentalization at single-embryo resolution.

Immunohistochemistry was performed according to established protocols. Embryos were blocked in 5% normal goat serum (NGS) in PBT (PBS with 0.3% Triton X-100) for 1 h at room temperature. Primary antibody incubation was performed overnight at 4°C using rabbit anti-Vasa antibody (a kind gift from Dr. Paul Lasko) at a 1:100 dilution in PBT with 1% NGS. After several washes in PBT, embryos were incubated with Alexa Fluor 555-conjugated goat anti-rabbit secondary antibody (Cell Signaling Technology, #4413) at a 1:500 dilution for 2 h at room temperature in the dark. Immunohistochemistry was performed to localize germline-associated proteins and to complement the spatial expression data obtained via HCR. By combining Vasa protein localization with *oskar* mRNA expression, we aimed to verify the germline identity of cells within the germline capsule.

2.6 | Marking of the Germline Capsule

To mark the germline capsule and determine whether its cellular components contribute to the developing gonads, we optimized a nucleotide-labeling approach based on DIG-dNTP incorporation. This method relies on the uptake and recycling of digoxigenin-labeled nucleotides into the DNA, allowing detection of nuclei that inherit labeled material during subsequent replication or DNA repair. If DNA originating from the capsule are transmitted to the presumptive gonad, the DIG signal should later appear within this region. Microinjection of digoxigenin-labeled nucleotides (DIG-dNTP mix, Roche) was performed on *C. floridanus* embryos with a solution containing 35 nM of labeled DIG-dNTP. For capsule-specific labeling, injections were carried out at stage 8, when the germline capsule is morphologically distinct, and injection was performed directly into the germline capsule using fine glass capillary needles mounted on a Narishige microinjection system. As a control, embryos were injected 1 day after egg laying, before cellularization (pre-syncytial stage). This control allowed diffuse

incorporation of DIG across the embryo, labeling a broad range of nuclei, including those of the presumptive gonad. Injected embryos were incubated at 25°C in humid chambers until stage 16 when the presumptine gonad discs form. Then, embryos were fixed as described above for in situ hybridization. DIG-labeled nuclei were detected using anti-DIG–alkaline phosphatase conjugate (Roche) and NBT/BCIP chromogenic substrate according to manufacturer instructions.

2.7 | Phylogenetic Analysis

A phylogenetic tree was constructed for 30 ant species, including 26 species reported by (Ward et al. 2025), two species from colonies maintained in our laboratory *C. sanctus* and *C. auriventris*, and two additional species *C. floridanus* and *C. pennsylvanicus*. Phylogenetic relationships among these taxa were estimated using genomic fragments identified from the data set of (Ward et al. 2025) as reference sequences for comparisons. From the Ward data set comprising 225 species, five consensus sequences ranging from 800 to 1600 base pairs in length were generated. Primers were designed based on these consensus sequences to amplify the corresponding genomic regions in species not represented in the original data set. For the species maintained in laboratory colonies, total RNA was extracted, cDNA was synthesized, and amplified products were sequenced using Sanger method (Sanger et al. 1977). Sequences from each target were aligned using MAFFT v7 (Katoh 2002), and three representative targets containing the 30 species were subsequently trimmed for unaligned regions, and concatenated into a single alignment of approximately 2000 base pairs. Phylogenetic reconstruction was performed using the maximum likelihood method implemented in PhyML v3.0 (Guindon et al. 2010). Among the resulting topologies, the tree most consistent with the reference phylogeny of (Ward et al. 2025) was selected.

2.8 | Preparation of cDNA Libraries for Transcriptomics

For transcriptomic analysis, embryos were staged and collected at two key developmental stages; stage 5 and stage 8. During stage 5, the germline capsule and bacteriocytes become morphologically distinguishable but are not yet separable. Therefore, whole embryos were collected at this stage to represent early capsule specification. By stage 8, both the germline capsule and bacteriocytes are morphologically distinct, allowing for manual dissection. Stage 8 samples were dissected under a stereomicroscope to isolate germline capsules, bacteriocytes. For clarity, later we analyzed the transcriptomes of the host and the endosymbiont separately.

Three biological replicates were prepared for each sample type. For stage 5, 10 whole embryos per replicate were directly pooled into TRIzol reagent (Thermo Fisher Scientific) without dissection. For stage 8, germline capsules and bacteriocytes were manually dissected from approximately 60 embryos per replicate under a stereomicroscope. Each tissue type was pooled separately into TRIzol for RNA extraction. Total RNA was isolated according to the manufacturer's protocol (Sigma). cDNA libraries were constructed using the ZYMO-seq RiboFree Total RNA Library Kit (Cat#R3000) following the manufacturer's guidelines.

2.9 | Data Processing

Sequencing was performed on the NovaSeq. 6000 platform using paired-end 150 bp sequencing. A single run generated approximately 6 GB of data, yielding around 40 million raw reads. The preprocessing of raw data received from new-generation sequencing was conducted using fastp (Chen 2023), which is an all-in-one tool for quality control, adapter and polyG trimming, low-quality read filtering, deduplication, and quality reporting. The filtered reads were then mapped to the reference genome of *C. floridanus* (GCF_003227725.1_Cflo_v7.5) (Shields et al. 2018) from NCBI (Sayers et al. 2023) using Kallisto software (Bray et al. 2016) for transcript quantification. The count data were imported with the tximport tool into R (v4.4.1) statistical software (Team 2023). Differential gene expression analysis was carried out using the DESeq. 2 package (Love et al. 2014) in R. Differentially expressed genes were identified using an adjusted *p*-value threshold of < 0.01 because in transcriptomic analyzes, an adjusted *p*-value is commonly applied—typically using a multiple testing correction method—to minimize the incidence of false positives in differential expression results. The absolute log2 fold-change ($|FC|$) > 1 was chosen to capture at least a two-fold expression. Functional enrichment analysis of these genes was performed using the DAVID bioinformatics tool (Sherman et al. 2022) with a significance threshold of $p < 0.05$, as in standard statistical analysis. After that, gene ontology (GO) terms and Kyoto Encyclopedia of Genes and Genomes (KEGG) pathways were analyzed to gain insights into the biological implications of gene expression changes. GO provides structured terms to describe gene functions in three domains: biological processes (BP), molecular functions (MF), and cellular components (CC). KEGG, on the other hand, maps genes to curated metabolic and signaling pathways. Together, these analyzes allow us to study the potential functional significance of transcriptomic changes observed in the germline capsule and associated tissues, and to identify candidate pathways potentially involved in its development and regulation. In addition, the filtered reads processed by fastp were mapped to the annotated genome of *C. Blochmannia* (GCA_000043285.1) using Bowtie2 software (Langmead and Salzberg 2012), and those mapped reads were counted with featurecounts in the Rsubread package (Liao et al. 2019). Subsequently, differential expression analysis was performed using DESeq. 2 in R. Visualization techniques, including heatmaps, principal component analysis, volcano plots, and functional enrichment graphs, were generated using R packages (ggplot2, pheatmap).

2.10 | Microscopy

Samples were placed onto a microscope slide in 75% glycerol and covered with a cover slip using spacers to avoid the crushing of embryos. Imaging was performed using Confocal Microscopy (Leica SP8) using the Diode 405 nm laser for DAPI, OPSL 488 nm for HCR, and OPSL 552 nm for immunostaining. The colorimetric in situ hybridization signals were visualized

and documented using a differential interference contrast microscope (Leica). We used 20X, 40X, and 40X oil immersion objectives. Raw image data were processed and analyzed using ImageJ Software version 2.15.1 (Rueden et al. 2017) and Adobe Illustrator.

3 | Results

3.1 | Function of the Germline Capsule

The germline capsule is a derived structure containing germ granule components that potentially replace or partially contribute to the ancestral posterior pole germline. To understand whether the the germline capsule actually replaces or contributes to the functional germline despite the presence of the ancestral germline, we experimentally marked the germline capsule using DIG-dNTP injection and at the same time followed its development in wildtype (unmarked) embryos using immunostaining for germline marker Vasa (Figure 1). Our results show that DIG-dNTP injected embryos that were injected explicitly in the germline capsule at stage 8 marked the presumptive gonad region in the posterior of the embryo (Figure 1a–a″, n/N = 6/30). In parallel, embryos injected in pre-syncytium stage marked a wider range of nuclei, including the presumptive gonad region (Figure 1b, n/N = 3/24).

At stage 1, Vasa staining was observed at the posterior pole of the egg and as a stripe at the anterior edge of the bacterial mass (Figure 1c,c'). At stage 2, Vasa became condensed at the posterior pole whileas the stripe appeared more ventrally condensed (Figure 1d,d'). At stage 5, the posterior Vasa expression was observed more internally within the bacteriocyte mass (Figure 1e,e'). At stage 8 Vasa expression in bacteriocyte mass appeared closer to the germ band; at this stage, the capsule is most clearly seen as a separate cell, with Vasa expression surrounding a cluster of presumptive germline nuclei (Figure 1f,f'). At stage 10, Vasa expression was positioned within the posterior of the germband, but the expression inside the bacteriocyte mass as well as the germline capsule was not detectable at stage 10 or onwards (Figure 1g,g'). The presumptive gonad expressed Vasa in these later stages (Figure 1h,h'). Together DIG and Vasa analysis revealed two Vasa-expressing foci in the posterior marking the ancestral germline and the nuclear cluster within the germline capsule, and suggest that the germline capsule contributes to the formation of the presumptive gonad.

3.2 | Molecular Features of the Germline Capsule

To understand the developmental origin of the germline capsule, we performed differential gene expression analysis between the capsule and its closest related cells, the

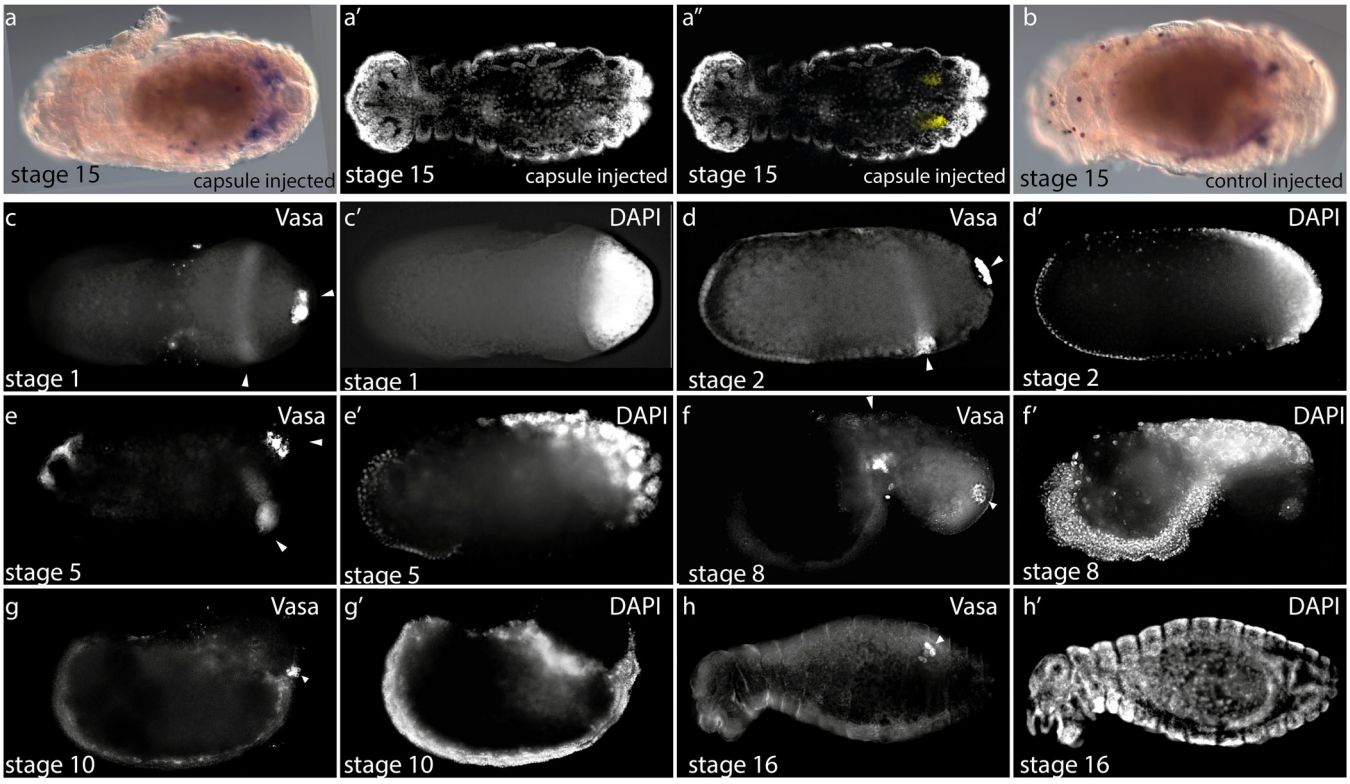

FIGURE 1 | Germline marked and Vasa immunostained embryos in the context of the developing capsule. (a–b) embryos of *C. floridanus* injected and stained with DIG labeled-dNTP, injected into the germline capsule at stage 8 (a–a"), or injected into the pre-syncytium (b). Note the blue staining in the gonad region in (a) is coincident with the gonad nuclei in (a') highlighted with yellow false color in (a"). (c–h) Embryos of *C. floridanus* immuno-stained with Vasa antibody (c–h) and DAPI (c'–h'). Early Stage 1 embryo (c, c'), Stage 2 embryo (d, d'), Stage 5 embryo (e, e'), Stage 8 embryo (f, f'), Stage 10 embryo (g, g'), and Stage 16 (h, h'). Anterior is to the left. a–b are dorsal views, c–h are lateral views. Note that expression in the posterior is relevant to the germline capsule whileas the expression in the anterior in the embryonic tissue and yolk (d, e) are not directly relevant to the development or evolution of the germline capsule. [Color figure can be viewed at wileyonlinelibrary.com]

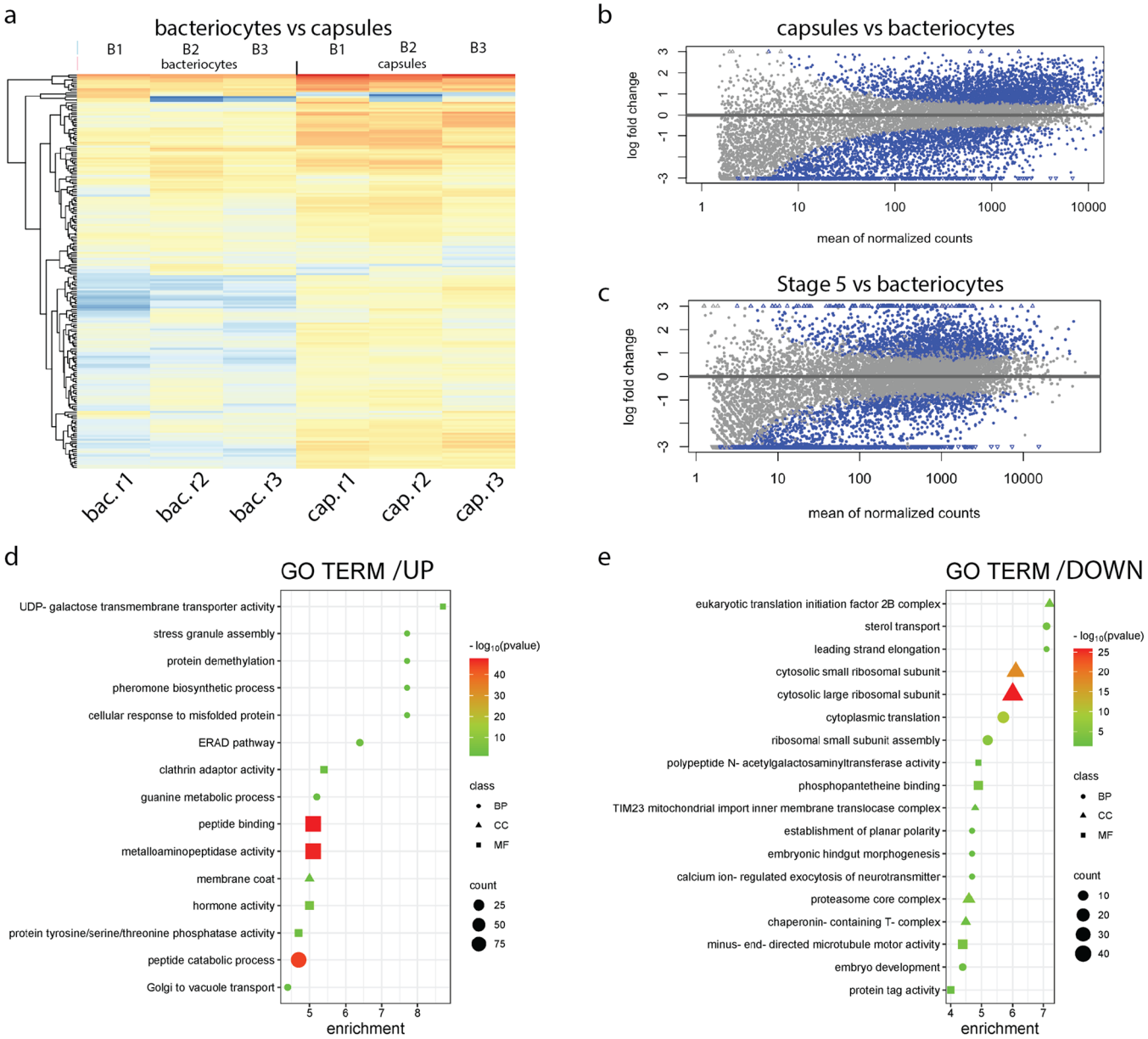

FIGURE 2 | Differential transcriptomic analysis of germline capsule vs bacteriocytes in *C. floridanus*. (a) Clustering of genes with similar expression profiles (left) and heatmap representing the genes color-coded according to their levels of expression from high (red) to low (blue) (right) in three samples each of bacteriocytes and capsules. (b and c) Volcano plots representing differential gene expression between, the germline capsules versus bacteriocytes (b), and whole embryos at stage 5 versus bacteriocytes (c). (d and e) Graphs representing functional gene enrichment in the germline capsule. GO terms related to upregulation (d), or downregulation (e) in the germline capsule retrieved from DAVID. Molecular function, cellular component, biological process are represented by shapes whose sizes represent the gene numbers involved. The color codes for panels (d and e) indicate high to low (red to green) Log_{10} *p*-values. Abbreviations: Batches and replicates are indicated. Batch 1 (B1) consists of bac.r1 and cap.r1, batch-2 (B2) consists of bac.r2 and cap.r2, batch-3 (B3) consists of bac.r3 and cap.r3. Note that batch effect was also considered. [Color figure can be viewed at wileyonlinelibrary.com]

bacteriocytes (Figure 2a–b, Supporting Information Figure S1). This approach allowed us to identify candidate genes and pathways potentially involved in capsule formation, including both upregulated and downregulated genes. The raw read numbers from the samples were in the range of 30 to 64 million reads, and the read numbers after data cleaning were in the range of 24 to 44 million reads (Supporting Information Table S1). Mapping of the cleaned transcriptome data from these samples to the reference genome of the host, when using 10 reads as a minimum cutoff, revealed that 11,563 genes were differentially expressed between the bacteriocyte and the germline capsule out of a total of 13462 genes. For the *p*-value of < 0.05, 1614 genes (14%) were upregulated, whereas 2425 genes (21%) were downregulated in the germline capsule. Refining the gene list by adding batch effect and selecting those with a $\log_2$Fold Change ($|FC|$) > 1 and an adjusted *p*-value of < 0.01 resulted in 1498 upregulated and 1540 downregulated genes for further analysis (Figure 2b).

Functional gene enrichment using Gene Ontology (GO) analysis in DAVID revealed that one of the most significant biological processes (BP) upregulated in the germline capsule was

proteolysis, involving 159 genes (FE = 2.2) (Supporting Information Table S2, Figure 2d). The high number of genes involved in proteolysis and catabolic processes of peptides (96 genes, FE = 4.8) indicates a strong focus on protein degradation, particularly via the proteasome pathway (18 genes, FE = 1.8). The highly functional enriched terms in this category are stress granule assembly (3 genes, FE = 8.1), pheromone biosynthesis (3 genes, FE = 8.1), and protein demethylation (3 genes, FE = 8.1). The most significant molecular functions (MF) were protein binding with 158 genes (FE = 1.2) and zinc ion binding with 148 genes (FE = 2). Among the enriched terms, transmembrane transporter (3 gene FE = 9.1), clathrin adapter (5 genes FE = 5.7), and SNARE binding (9 genes FE = 3.0) got the highest score. When GO terms were examined for enrichment of cellular components (CC), 47 genes were found to be associated with the endoplasmic reticulum membrane (FE = 1.4), 36 with the endoplasmic reticulum (FE = 1.8), 23 with the Golgi apparatus (FE = 1.5), and 17 with lysosomes (FE = 1.9), indicating active cell trafficking processes. At the same time, KEGG pathway analysis identified Glutathione metabolism as the most significantly upregulated pathway, which included 63 participating genes (FE = 3.8). Additionally, it identified autophagy (70 genes, FE = 2.5) and Lysosome (65 genes, FE = 2.3). These findings reveal that proteolysis, intracellular trafficking, cell adhesion, and stress response are the hyperactively ongoing processes in the germline capsule when compared to its nearest neighboring cell type, the bacteriocyte.

On the other hand, using the DAVID clustering algorithm, the genes that were shown as downregulated in the germline capsule indicate that ribosomal activity and protein synthesis are the most reduced in the germline capsule (Supporting Information Table S2, Figure 2e). In agreement with this, the biological process (BP) GO terms revealed that the most downregulated process was translation (77 genes, FE = 3.9), followed by cytoplasmic translation with 17 genes (FE = 6.9), and translational initiation with eight genes (FE = 3.4). These were followed by the ribosomal process, such as ribosome biogenesis (11 genes, FE = 4.3), ribosomal small subunit assembly (11 genes, FE = 6.3), and ribosomal large subunit assembly (7 genes, FE = 3.2). Similar to these results, the GO terms for molecular function (MF) were, in order of significance level: the structural constituent of ribosome (94 genes, FE = 4.1), the structural constituent of chromatin (13 genes, FE = 4.3), RNA binding (74 genes, 1.6), DNA binding (68 genes, 1.4), ATP binding (120 genes, FE = 1.2), protein folding (154 genes, 1.1), and DNA-dependent RNA polymerase activity (7 genes, FE = 3.7). The cellular component (CC) of GO terms retrieved: ribosome (87 genes, FE = 4.2), and mitochondrion (59 genes, FE = 1.3) (Supporting Information Table S2). These results can be interpreted as an overall reduction of cell metabolic activities in the capsule, in comparison to the bacteriocytes.

During the earliest stage of zygotic genome activation—before the visible formation of the germline capsule—166 genes that are later upregulated in the germline capsule were already transcriptionally upregulated in the whole embryo (Figure 2c, Supporting Information Table S3). Conversely, at the same stage, 690 genes were downregulated in the entire embryo from among the genes downregulated in the germline capsule (Figure 2c, Supporting Information Table S3). DAVID analysis of these gene lists revealed that the constitutively hyperactive processes in embryogenesis compared to the bacteriocyte data set were proteolysis (22 genes, FE = 2.9), zinc-ion binding (24 genes, FE = 3.0), pheromone (2 genes, FE = 49.9), and nucleosome complex (4 genes, FE = 20.3). On the other hand, the downregulated processes were translation (51 genes, FE = 7.0), plasma membrane (65 genes, FE = 1.4), cell differentiation (12 genes, FE = 2.6), BMP binding (3 genes, FE = 16.6), and cytoskeletal movement with microtubule and dynein (10 genes, FE = 3.1, six genes, FE = 6.6, respectively). Together, these results indicate that while some capsule-specific genes are transcriptionally primed before capsule formation, others are uniquely activated during its maturation, highlighting a two-phase regulatory program underlying capsule development.

To test whether bacterial gene expression also differed between the germline capsule and bacteriocytes, given that both harbor substantial populations of *Blochmannia*, we investigated the expression of the endosymbiont genome. Differential expression analysis using DESeq. 2 on 631 genes across six samples showed that only three genes, all components of structural RNA, were significantly upregulated in the capsule. In contrast, no genes were significantly downregulated (adjusted $p < 0.01$). These results indicate that bacterial gene expression is consistent mainly between the two tissue types, with minimal transcriptional divergence observed under the conditions tested (Supporting Information Figure S2).

3.3 | Cellular Structure of the Germline Capsule

While transcriptomic analysis provided hints into the molecular landscape of the germline capsule, understanding the cellular basis of these differences required detailed morphological examination (Figure 3). During the blastoderm stage of the embryo at stage 5, the presumptive region, which eventually forms the germline capsule, is in the region immediately anterior to the bacteriocytes, at about 80% egg length (taking the anterior as 0%), and a row of nuclei can be observed (Figure 3a–f). These nuclei, which first appeared in the syncytium, were enveloped within a line of cells across the ventral side in cellularized embryos (Figure 3a). The nuclei within these cells were seen as clusters of progressively higher numbers of nuclei progressively turning into a a larger cell, bigger than any neighboring cell, between stages 5 and 7 (Figure 3b–f). The diameter of the single cluster of nuclei was about 55. 7 micrometers, and that of a single nucleus within it was about 11.6 micrometers. For reference, the germline capsule diameter on average is 172.2 micrometers, while that of the bacteriocyte is 42.8 micrometers. From this data, we infer that a row of cells fuses to form the germline capsule (compare Figure 3a,f). At all stages of development—be it as a syncytial row of nuclei, individual germline cells, or a mature germline capsule—the expression of the germline determinant *oskar* persists, and bacteria are consistently localized near the germline nuclei (Figure 3g–i). The morphological analysis hints to the involvement of cell-cell fusion in the formation of the germline capsule.

3.4 | Bacterial Influence on the Phenotype of Germline Capsule

While analyzing multiple embryos, we observed a few exceptions to the stereotypical phenotype (Figure 4). In some, the

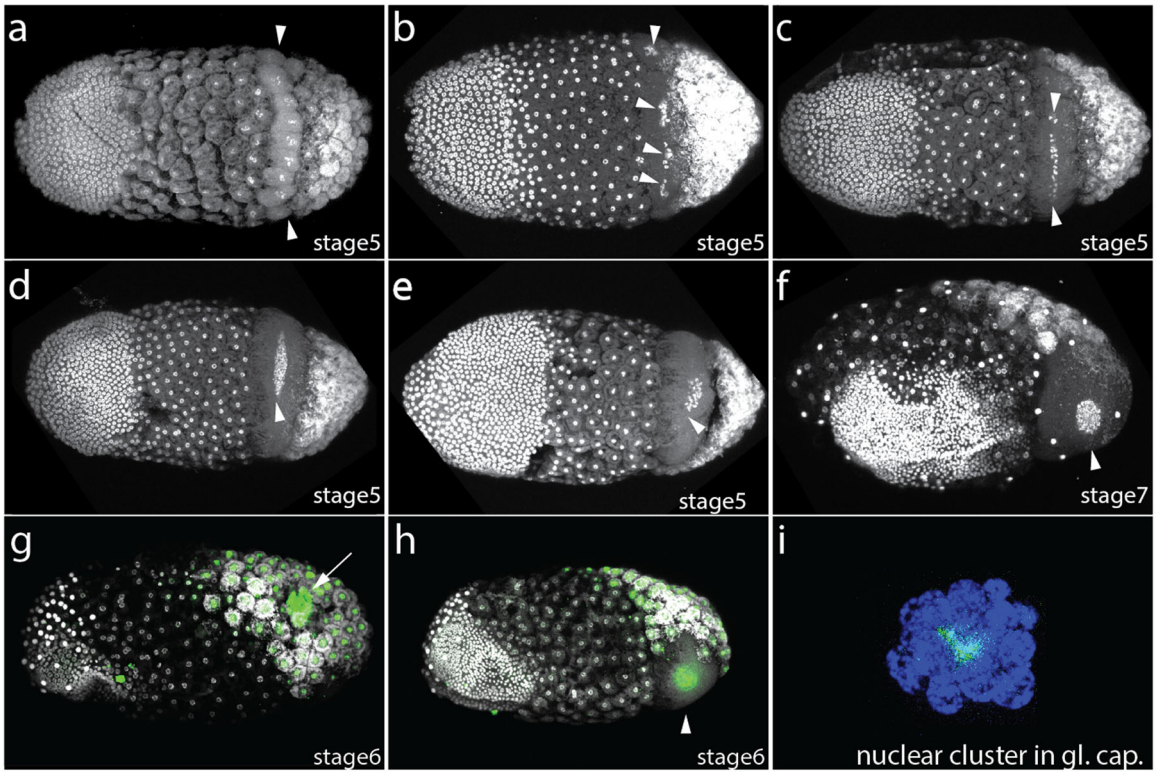

FIGURE 3 | Formation of the germline capsule during early embryonic development in *C. floridanus*. (a–f) Confocal microscopy images showing the distribution of host cell nuclei, bacteria, and the overall embryo structure in relation to the germline capsule. A row of cells containing multiple host nuclei is observed anterior to the bacteriocytes (a). As the embryo develops, these cells fuse and their nuclei gradually move closer to one another (b–e). In most embryos by Stage 7, the germline capsule acquires its final spherical shape, with the nuclear cluster fully assembled inside (f). (g–h) An embryo showing *oskar* expression from two perspectives (g and h); showing the ancestral germline located within the bacteriocyte mass (arrow in g) and the novel germline, located within the capsule (arrowhead in h). (i) A close-up view of the cluster of germline nuclei inside the germline capsule expressing *oskar*. Arrowheads indicate the nuclei inside the capsule. Embryos (a–e) are ventrally oriented, (f and h) are ventrolaterally oriented, whileas (g) is dorsolaterally oriented. Anterior is to the left. Note hybridization chain reaction with a probe against *oskar* (green), and nuclear stain DAPI (white) except blue in (i). [Color figure can be viewed at wileyonlinelibrary.com]

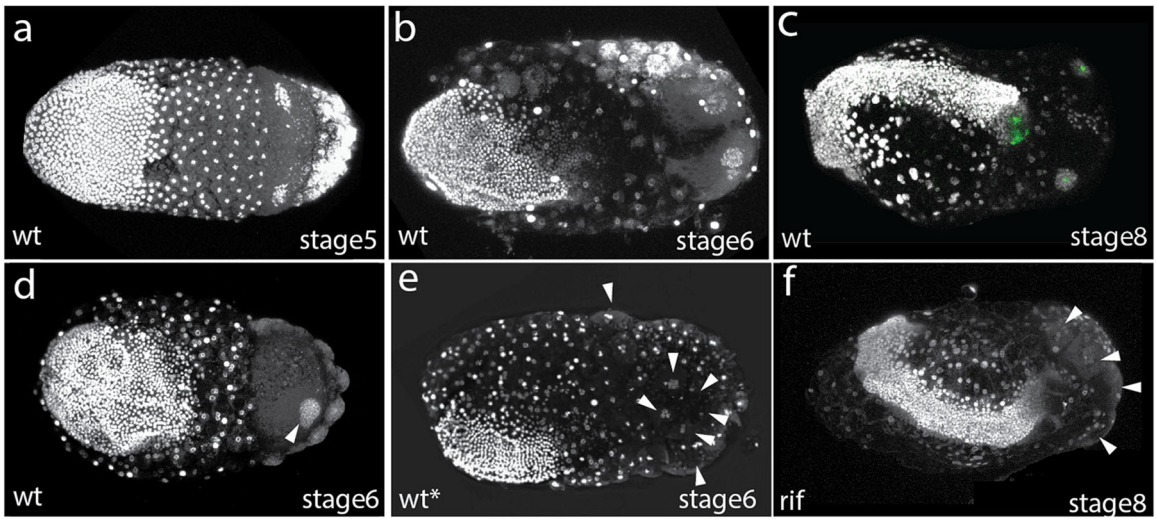

FIGURE 4 | Developmental plasticity of the germline capsule in response to bacterial load. (a–c) Embryos of *C. floridanus* of different embryonic stages and bacterial loads exhibiting the two germline capsule phenotype along with the cluster of germline nuclei (a–c) additionally displaying *oskar* expression in both the ancestral germline and the two germline capsules (c). (d) A single germline capsule forms in majority of embryos. (e–f) More than one capsule forms in an older colony with a reduced bacterial load (e) or after antibiotic treatment (f). Arrowheads indicate the germline capsule. Panels (a and d) are ventrally oriented, (b, e, f) are ventrolaterally oriented, and (c) is dorsolaterally oriented. Anterior is to the left. rif, rifampicin treated; wt, wildtype; wt*, from an older colony. Nuclear stain DAPI (white) and *oskar* HCR (green) are shown. [Color figure can be viewed at wileyonlinelibrary.com]

germline capsule did not form a single structure but was further compartmentalized into two identical capsules or two capsules of different sizes (Figure 4a,b), each of which contained characteristics of a germline capsule in the shape of a cluster of germline nuclei and expression of *oskar* mRNA surrouding them ($n = 6/100$) (Figure 4c). Furthermore, embryos from multiple colonies also showed these 'twin capsules' in as many colonies as we tested. Nonetheless, the frequency of two capsules appeared to be a repeatable phenotype of the germline capsule. In one of the colonies, which was exceptionally older (~12 years) we observed embryos with gradually lesser and lesser bacteria until they stopped having any. These embryos consistently developed multiple capsules (Figure 4e) compared to wildtype (Figure 4d). To figure out whether bacteria influence the variation in germline capsule phenotype, we manipulated the number of endosymbiotic bacteria through antibiotic treatment. Consistent with previous studies (Rafiqi et al. 2020), we observed that depletion of bacteria led to a phenotype where multiple capsules were formed in addition to one or two (Figure 4f). Germline gene expression profiles and phenotypic differences between wild-type and antibiotic-treated colonies of *C. floridanus* suggest that the germline capsule phenotype is influenced by microenvironmental factors, such as bacterial presence.

3.5 | Phylogenetic Distribution and Phenotypic Variation in the Germline Capsule

The germline capsule is uniquely described for species in the genus *Camponotus*. Ants outside of this genus have not been reported to consist of a similar structure to the best of our knowledge. To contexualize the germline capsule we surveyed as many species as we could obtain and for which morphological data was previously described (Figure 5, Supporting Information Figure S3). The sister genera of *Camponotus*; that is *Colobopsis* and *Polyrhachis* both lack a germline capsule, but contain bacteriocytes in the posterior (Figure 5b,c). Our reconstruction of the phylogeny reveals four clades within genus *Camponotus*: First one consists of *C. americanus*, and *C. pennsylvanicus*; a second one consists of *C. festinatus* and *C. floridanus*; a third clade consists of *C. nicobarensis*, and two highly similar species closely related *C. baldacci and C. sanctus*; and a fourth clade represented by a single species in our sample *C. auriventris* (Figure 5a). We then analyzed the morphology of the species of our sampling, where the presence or absence of a germline capsule was unknown. Within the genus *Camponotus*, of the eight where the morphology was already described, we added four more species to the list and report the germline capsule as present in eight of the species and absent in four of them (Figure 5d–i). Together, these data indicate multiple gains and losses of the germline capsule have occurred within the genus *Camponotus*.

To test whether the species exhibiting a germline capsule, share the germline function in this structure, we analyzed *oskar* gene expression in different species that have or do not have the germline capsule (Figure 6). In *Colobopsis*, *oskar* expression is restricted to the single germline present within the mass of bacteriocytes in the posterior (Figure 5b). Similar to *C. floridanus*, all *Camponotus* species examined showed *oskar* expression in every bacteriocyte (Figure 5d, Figure 6c,e), unexpectedly for cells that evade germline fate. Furthermore, in *Camponotus* species with a germline capsule, *oskar* marks the nuclear cluster inside this cell, with the only exception of *C. auriventris* in our sampling (compare Figure 3h,i and Figure 5d with Figure 6h,k). In *C. auriventris*, *oskar* was expressed in the posterior region of the embryo at an early stage (Figure 6f). At a later stage (cellularization), the *oskar* mRNA was expressed around a cluster of germline nuclei placed within the bacteriocyte mass (Figure 6g,g',g",g"'). With cellularization, germline nuclei changed their position within the bacteriocyte mass from the surface deeper, and continued to express *oskar* (Figure 6i,j). A large capsule was formed at the anterior proximity of the bacteriocyte mass (Figure 6h,k). Interestingly, the capsule in *C. auriventris*, did not exhibit two characteristics of the germline capsule compared to other species: The nuclei within the capsule were loosely clustered, and the expression of *oskar* was not detectable within our methodological limits (Figure 6h). In *C. nicobarensis*, on the other hand, rod-shaped bacteria were also located in the posterior position of the egg, similarly. Germline nuclei were observed in the posterior position in early embryos (Figure 6a). In stage 8 embryos, they were observed in a location within the mass of bacteriocytes (Figure 6d). Although we did not find a germline capsule, we found the expression of germline genes in the posteriorly originating ancestral germline nuclei and in the bacteriocytes. Interestingly, the most anteriorly placed bacteriocytes, which expressed *oskar* mRNA, also exhibited the presence of very low bacterial load and centrally placed nuclei (Figure 6d,d',d",d"'). Both of these features resemble the germline capsule of *C. floridanus* in its initiation phase (compare Figure 3a with Figure 6d–d"'). These data show that *oskar* is universally expressed in the bacteriocytes of genus *Camponotus*, whether they have a germline function or not. They also show that *oskar* is expressed in the germline capsule, with the exception of one species. Finally, in one of the species *C. nicobarensis* we demonstrate that a low bacterial load in the bordering bacteriocytes, correlates with the centralized subcellular localization of the nuclei and *oskar* expression.

4 | Discussion

The germline capsule is a single large multi-nucleated cell, the likeness of which has not been described in any other ant embryos outside of specific lineages in the genus *Camponotus*. The unique structure, size, composition, and potential novel function as germline make the germline capsule a highly likely case of an evolutionary novelty.

Morphological analysis suggests that a row of cells of the embryo fuses to create a large, multinucleated germline capsule, a formation which possibly involves a specific cell-cell fusion event during early embryogenesis (Chen and Olson 2005). The early expression of germline genes in these rows of cells may facilitate the formation of the germline capsule through the splitting and fusion dynamics characteristic of liquid–liquid phase separation of germplasm (Brangwynne et al. 2009; Hnisz et al. 2017). This cell–cell fusion might be required to organize the germline as a single compartment in the germline capsule. Consistent with this, the experimental marking of germline capsule indicates that the capsule contains germ granule

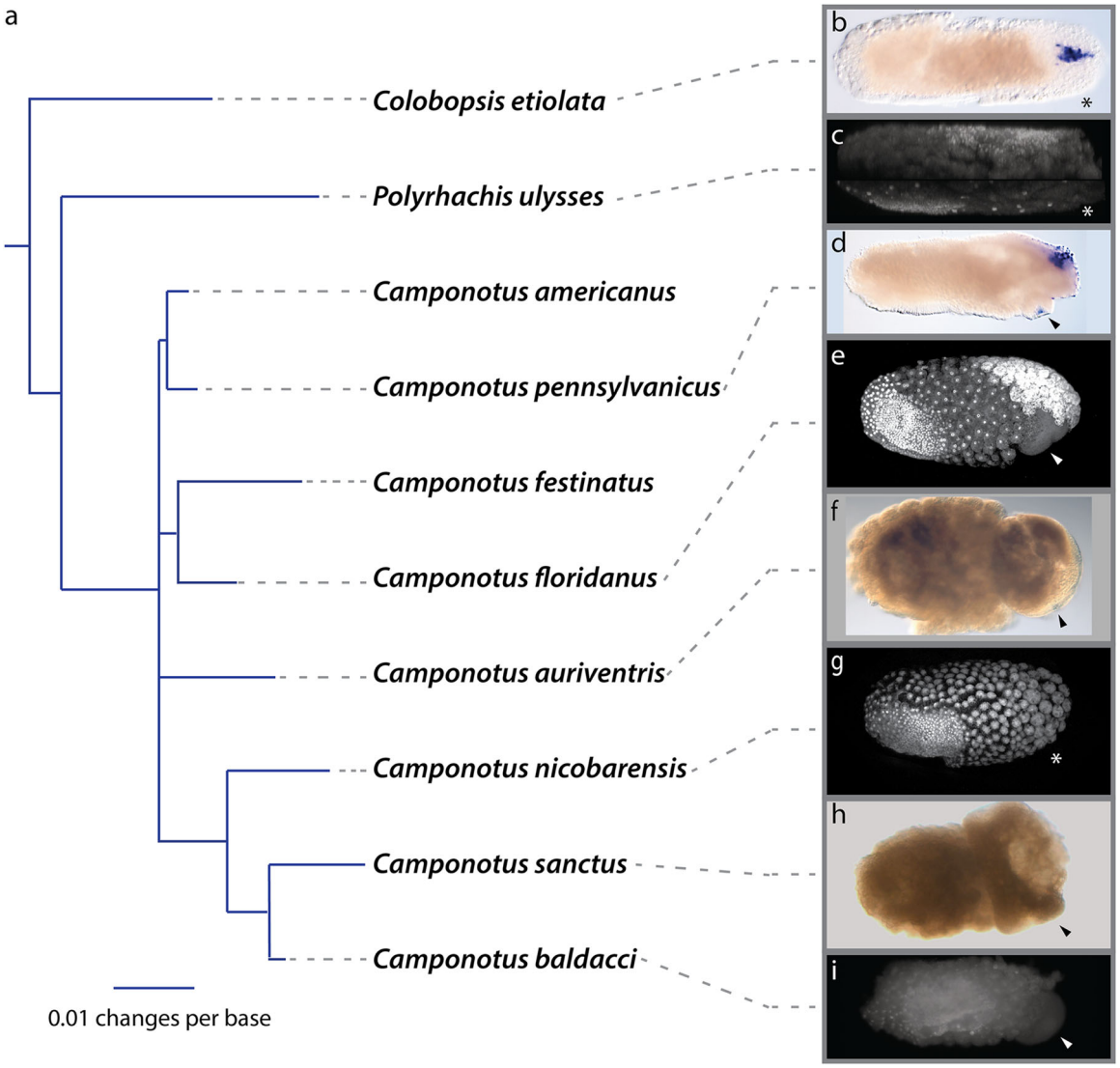

FIGURE 5 | Phylogenetic relationship between ants of the tribe Camponotini with the distribution of germline capsule. (a) Graphical representation of PhyML tree obtained from 2000 bp DNA bases. (b-i) Microscopic images of embryos from different species showing the presence (arrowhead) and absence (asterisk) of the germline capsule. (b, d) are in situ hybridized with a probe against *oskar* mRNA, (c) is a combined 3D projection from DAPI stained aspects of the same embryo, (e, g, and i) are DAPI stained embryos, whileas (b, d, f, and h) are DIC images. Blue branches are obtained from the PhyML (scale shown at the bottom left), while gray dashed lines are arbitrary. Note that the germline capsule is present in *C. americanus* and absent in *C. festinatus*. [Color figure can be viewed at wileyonlinelibrary.com]

components and transmits germline to the presumptive gonad despite the persistence of an ancestral germline at the posterior pole. This means that the capsule functionally participates in establishing the germline, potentially representing a derived mechanism that partially contributes to or replaces the ancestral posterior germline in *C. floridanus*.

Components of the endomembrane system are hyperactive in the maturing germline capsule, which indicates a coordinated enhanced intracellular trafficking and vesicle formation (Brandizzi and Barlowe 2013; Chen and Olson 2005). Given our proposal that germline is transmitted from the capsule to the presumptive gonads, this molecular signature suggests that endomembrane components may actively participate in coordinating the packaging, movement, and targeted delivery of germline during early development. Apart from these findings, the upregulation of glutathione metabolism indicates an intense oxidative stress response, a condition often representing a critical threshold between cell survival and programmed cell death (Fulda et al. 2010). In parallel, the induction of autophagy and lysosomal pathways points to active degradation processes within the germline capsule. These signatures, along with the global downregulation of transcriptional and translational activity, are consistent with a stress-induced dismantling of the capsule starting at stage 8. Together, these observations suggest that the germline capsule undergoes a tightly regulated transition at stage 8, balancing active germline packaging and transport with stress-induced degradation processes that mark the onset of its disassembly.

In *C. floridanus*, we have observed multiple phenotypic outcomes of the germline capsule: A single germline capsule is the most frequently observed phenotype (roughly 94%) compared to two capsules (~6%) or multiple capsules (old queens). This suggests

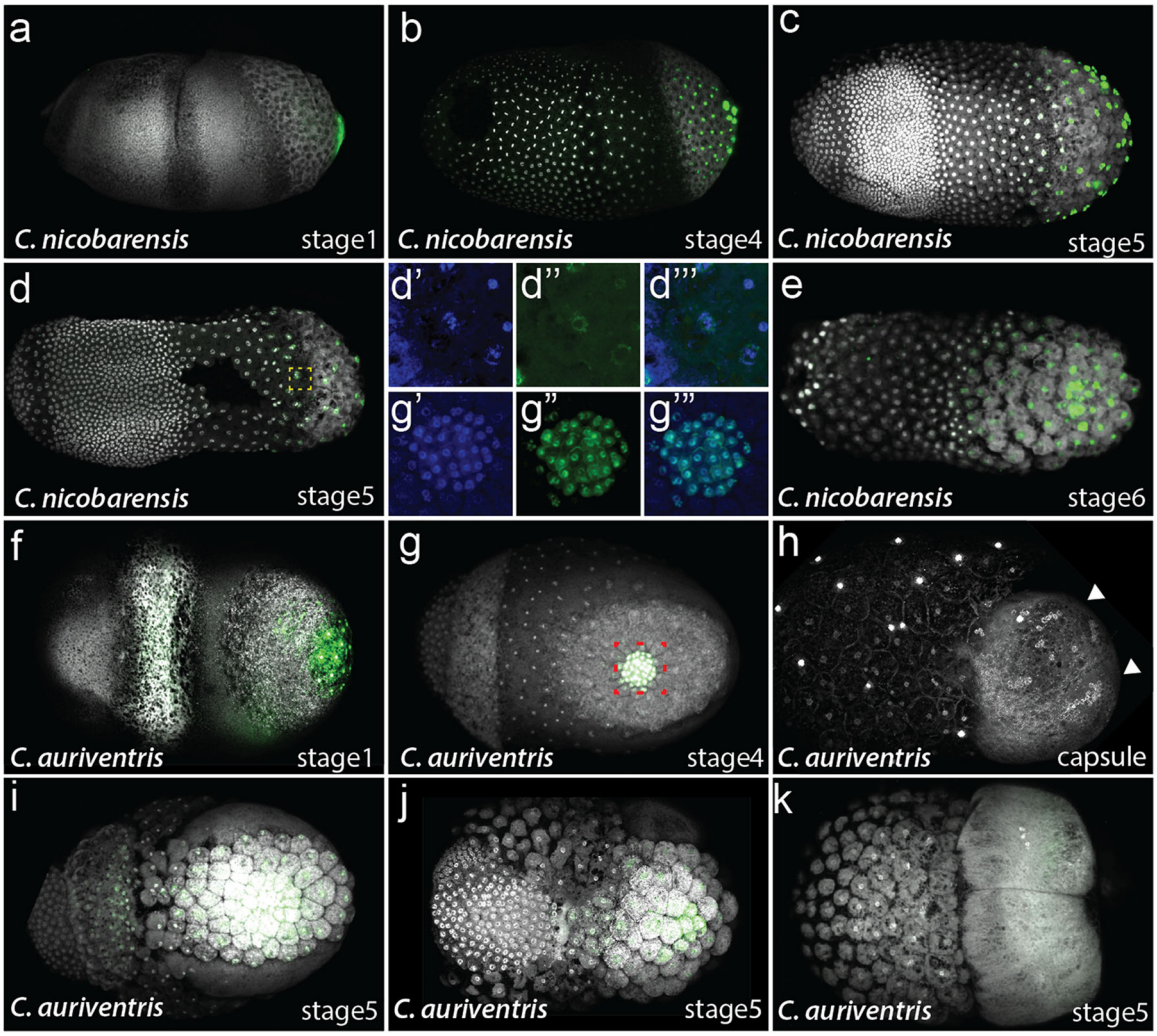

FIGURE 6 | Comparative analysis of germline capsule formation and *oskar* expression in different *Camponotus* species. (a–e) In *C. nicobarensis*, germline nuclei are localized at the posterior in the early embryo (a). In later embryos, these nuclei are found within the bacteriocyte mass, with *oskar* expressed in both germline nuclei and bacteriocytes (b–d). Anterior-most bacteriocytes express *oskar*, and exhibit low bacterial load (d–d'''). (f–k) In *C. auriventris*, *oskar* is expressed in the posterior region at early stages (f). During cellularization, germline nuclei continue to express *oskar* as they migrate within the bacteriocyte mass (g–g'''). Individual bacteriocytes also show low-level *oskar* expression (g, i, j). A large germline capsule with loosely clustered nuclei, indicated by arrowheads, lacking *oskar* expression is shown (h). In some embryos, two separate germline capsules form (k). Panels (a, b) are lateral views, (c, d, h, and k are ventral, (e, f, g, i, and j) are dorsal views. Anterior is to the left. HCR against *oskar* mRNA (green), and nuclear stain DAPI (white) are shown. DAPI is exceptionally shown colored in d', d''' and g', g''' (blue). [Color figure can be viewed at wileyonlinelibrary.com]

that the single capsule is the representative phenotype, while the other two alternatives are states of variation of this phenotype. The observation of multiple capsules after the removal of bacteria through antibiotic treatment or natural loss of bacteria in old colonies suggests that capsule development can be successfully initiated by the host genes in the absence of bacteria, but frequently fails to form a multinucleated single cell. Although the variation in capsule morphology could arise from underlying genetic differences (Charlesworth et al. 1982; Hoekstra 2006), it more likely reflects environmentally induced developmental plasticity, because the phenotype appears to be influenced by bacterial presence. Although bacterial transcripts did not show any significant differences between the bacteriocytes and germline capsules, the observations from treatments and older colonies suggest that bacterial endosymbionts provide a local microenvironment that potentially stabilizes capsule morphogenesis.

Comparative analysis of *oskar* expression in different species revealed how germline function evolved within the genus *Camponotus* through bacteria-germline interaction. In *C. nicobarensis*, which does not form a germline capsule, *oskar* gene expression was present in bacteriocytes but appeared distinct in the anterior-most bacteriocyte cells, where bacterial density was comparatively low. Low bacterial density is reminiscent of the germline capsule in *C. floridanus*, suggesting that these cells are not entirely bacteriocytes and may contain a developmental potential to evolve into a germline capsule. However, this species lacks a germline capsule because the row of cells with the characteristics of germline capsule may not have the ability to undergo cell-cell fusion.

Based on our data we present a tentative model in which we postulate that the evolution of the germline capsule in

Camponotus is intimately linked to the acquisition of endosymbiosis. After the aquisition of the endosymbiont, Camponotini ants continued to express *oskar* at the posterior pole similar to the other ants. However, in species within the genus *Camponotus*, *oskar* expression expanded into bacteriocytes, suggesting a co-option of germline molecular components into endosymbiont-associated cells. Within this context, certain bacteriocyte boundary cells, characterized by reduced bacterial load, appear to represent transitional intermediates with regard to *oskar* expression. During the course of evolution, these newly specified germline gene-expressing cells exhibit a strong tendency to cluster and fuse, giving rise to a single multinucleated structure, the germline capsule. We suspect that some species may have initiated Vasa expression and other germline determinants, in the boundary cells, to facilitate the next step in germline capsule evolution. Examples of such Vasa expression will be interesting to explore in the future. Our model shows an example of an evolutionary novelty in the germline facilitated by the presence of endosymbiotic bacteria. It therefore paves the way for a deeper understanding of the evolution of novelty, and the role of cellular microenvironment and plasticity in this process.

Author Contributions

Z.Ö.D. and A.M.R. conceived the idea, Z.Ö.D. and N.S.M. conducted the experiments, A.R. performed Vasa immuno-staining, Z.Ö.D., N.S.M., A.M.R. wrote the manuscript.

Acknowledgments

We would like to thank the Scientific and Technological Research Council of Türkiye (TÜBİTAK) for the support awarded to AMR grant#120C157, Bezmialem Vakıf University BAP grant #20200822.

Conflicts of Interest

The authors declare no conflicts of interest.

Data Availability Statement

The details of the transcriptomic analysis are available at the GitHub Repository https://github.com/ZellOz/RNAseq---C.fl. The data of the transcriptome of different samples are in SRA PRJNA1370284.

References

Abouheif, E., M.-J. Favé, A. S. Ibarrarán-Viniegra, M. P. Lesoway, A. M. Rafiqi, and R. Rajakumar. 2014. "Eco-Evo-Devo: The Time Has Come." In *Ecological Genomics: Ecology and the Evolution of Genes and Genomes*, edited by C. R. Landry and N. Aubin-Horth, 107–125. Springer Netherlands. https://doi.org/10.1007/978-94-007-7347-9_6.

Bhatkar, A., and W. H. Whitcomb. 1970. "Artificial Diet for Rearing Various Species of Ants." *Florida Entomologist* 53: 229–232.

Brandizzi, F., and C. Barlowe. 2013. "Organization of the ER–Golgi Interface for Membrane Traffic Control." *Nature Reviews Molecular Cell Biology* 14, no. 6: 382–392.

Brangwynne, C. P., C. R. Eckmann, D. S. Courson, et al. 2009. "Germline P Granules are Liquid Droplets That Localize by Controlled Dissolution/Condensation." *Science* 324, no. 5935: 1729–1732.

Bray, N. L., H. Pimentel, P. Melsted, and L. Pachter. 2016. "Near-Optimal Probabilistic RNA-Seq Quantification." *Nature Biotechnology* 34, no. 5: 525–527.

Charlesworth, B., R. Lande, and M. Slatkin. 1982. "A Neo-Darwinian Commentary on Macroevolution." *Evolution* 36, no. 3: 474–498.

Chen, E. H., and E. N. Olson. 2005. "Unveiling the Mechanisms of Cell-Cell Fusion." *Science* 308, no. 5720: 369–373. https://doi.org/10.1126/science.1104799.

Chen, S. 2023. "Ultrafast One-Pass FASTQ Data Preprocessing, Quality Control, and Deduplication Using FASTP." *Imeta* 2, no. 2: e107.

Chen, T., A. M. Rafiqi, A. Rajakumar, et al. 2025. "A Developmental Table for the Florida Carpenter Ant *Camponotus floridanus*: establishing foundations for mechanistic studies of development and evolution in Ants." *Qeios Preprint*. Qeios.doi:10.32388/OJQC0N.

Choi, H. M. T., M. Schwarzkopf, M. E. Fornace, et al. 2018. "Third-Generation In Situ Hybridization Chain Reaction: Multiplexed, Quantitative, Sensitive, Versatile, Robust." *Development* 145, no. 12: dev165753.

Davidson, E. H., and D. H. Erwin. 2006. "Gene Regulatory Networks and the Evolution of Animal Body Plans." *Science* 311, no. 5762: 796–800.

Ephrussi, A., and R. Lehmann. 1992. "Induction of Germ Cell Formation by Oskar." *Nature* 358, no. 6385: 387–392.

Erwin, D. H. 2021. "A Conceptual Framework of Evolutionary Novelty and Innovation." *Biological Reviews* 96, no. 1: 1–15.

Extavour, and C. G. Akam. 2003. "Mechanisms of Germ Cell Specification Across the Metazoans: Epigenesis and Preformation." *Development* 130, no. 24: 5869–5884.

Fulda, S., A. M. Gorman, O. Hori, and A. Samali. 2010. "Cellular Stress Responses: Cell Survival and Cell Death." *International Journal of Cell Biology* 2010, no. 1: 1–23.

Galis, F. 2001. "Key Innovations and Radiations." In *Character Concept in Evolutionary Biology*, edited by G. F. Wagner, 25, 581–605.

Garcia-Fernàndez, J., and P. W. H. Holland. 1994. "Archetypal Organization of the Amphioxus Hox Gene Cluster." *Nature* 370, no. 6490: 563–566.

Gilbert, S. F., T. C. G. Bosch, and C. Ledón-Rettig. 2015. "Eco-Evo-Devo: Developmental Symbiosis and Developmental Plasticity as Evolutionary Agents." *Nature Reviews Genetics* 16, no. 10: 611–622. https://doi.org/10.1038/nrg3982.

Guindon, S., J.-F. Dufayard, V. Lefort, M. Anisimova, W. Hordijk, and O. Gascuel. 2010. "New Algorithms and Methods to Estimate Maximum-Likelihood Phylogenies: Assessing the Performance of Phyml 3.0." *Systematic Biology* 59, no. 3: 307–321.

Hnisz, D., K. Shrinivas, R. A. Young, A. K. Chakraborty, and P. A. Sharp. 2017. "A Phase Separation Model for Transcriptional Control." *Cell* 169, no. 1: 13–23.

Hoekstra, H. E. 2006. "Genetics, Development and Evolution of Adaptive Pigmentation in Vertebrates." *Heredity* 97, no. 3: 222–234.

Katoh, K. 2002. "MAFFT: A Novel Method for Rapid Multiple Sequence Alignment Based on Fast Fourier Transform." *Nucleic Acids Research* 30, no. 14: 3059–3066.

Khila, A., and E. Abouheif. 2008. "Reproductive Constraint Is a Developmental Mechanism That Maintains Social Harmony in Advanced Ant Societies." *Proceedings of the National Academy of Sciences* 105, no. 46: 17884–17889.

Khila, A., and E. Abouheif. 2009. "In Situ Hybridization on Ant Ovaries and Embryos." *Cold Spring Harb Protoc* 4, no. 7: 1–5.

Langmead, B., and S. L. Salzberg. 2012. "Fast Gapped-Read Alignment With Bowtie 2." *Nature Methods* 9, no. 4: 357–359.

Liao, Y., G. K. Smyth, and W. Shi. 2019. "The R Package Rsubread is Easier, Faster, Cheaper and Better for Alignment and Quantification of RNA Sequencing Reads." *Nucleic Acids Research* 47, no. 8: e47.

Love, M. I., W. Huber, and S. Anders. 2014. "Moderated Estimation of Fold Change and Dispersion for RNA-Seq Data With Deseq. 2." *Genome Biology* 15: 550.

McFall-Ngai, M., M. G. Hadfield, T. C. G. Bosch, et al. 2013. "Animals in a Bacterial World, a New Imperative for the Life Sciences." *Proceedings of the National Academy of Sciences* 110, no. 9: 3229–3236.

Moczek, A. P., S. Sultan, S. Foster, et al. 2011. "The Role of Developmental Plasticity in Evolutionary Innovation." *Proceedings of the Royal Society B: Biological Sciences* 278, no. 1719: 2705–2713.

Montgomery, M. K., and M. McFall-Ngai. 1994. "Bacterial Symbionts Induce Host Organ Morphogenesis During Early Postembryonic Development of the Squid *Euprymna Scolopes*." *Development* 120, no. 7: 1719–1729.

Müller, G. B., and S. A. Newman. 2005. "The Innovation Triad: An EvoDevo Agenda." *Journal of Experimental Zoology Part B: Molecular and Developmental Evolution* 304, no. 6: 487–503.

Pamula, M. C., and R. Lehmann. 2024. "How Germ Granules Promote Germ Cell Fate." *Nature Reviews Genetics* 25, no. 11: 803–821.

Pigliucci, M. 2008. "What, if Anything, Is an Evolutionary Novelty?" *Philosophy of Science* 75, no. 5: 887–898. https://doi.org/10.1086/594532.

Rafiqi, A. M., S. Lemke, and U. Schmidt-Ott. 2011. *Megaselia abdita*: Fixing and Devitellinizing Embryos. *Cold Spring Harb Protoc*, *2011*, pdb. prot5602.

Rafiqi, A. M., P. G. Polo, N. S. Milat, et al. 2022. "Developmental Integration of Endosymbionts in Insects." *Frontiers in Ecology and Evolution* 10: 846586.

Rafiqi, A. M., A. Rajakumar, and E. Abouheif. 2020. "Origin and Elaboration of a Major Evolutionary Transition in Individuality." *Nature* 585, no. 7824: 239–244.

Rajakumar, A., L. Pontieri, R. Li, et al. 2024. "From Egg to Adult: A Developmental Table of the Ant *Monomorium Pharaonis*." *Journal of Experimental Zoology Part B: Molecular and Developmental Evolution* 342, no. 8: 557–585.

Rueden, C. T., J. Schindelin, M. C. Hiner, et al. 2017. "ImageJ2: ImageJ for the Next Generation of Scientific Image Data." *BMC Bioinformatics* 18: 529.

Saffman, E. E., and P. Lasko. 1999. "Germline Development in Vertebrates and Invertebrates." *Cellular and Molecular Life Sciences* 55: 1141–1163.

Sanger, F., S. Nicklen, and A. R. Coulson. 1977. "DNA Sequencing With Chain-Terminating Inhibitors." *Proceedings of the National Academy of Sciences* 74, no. 12: 5463–5467.

Santos, A. C., and R. Lehmann. 2004. "Germ Cell Specification and Migration in Drosophila and Beyond." *Current Biology* 14, no. 14: R578–R589.

Sayers, E. W., J. Beck, E. E. Bolton, et al. 2023. "Database Resources of the National Center for Biotechnology Information." *Nucleic Acids Research* 52, no. D1: D33–D43.

Sherman, B. T., M. Hao, J. Qiu, et al. 2022. "DAVID: A Web Server for Functional Enrichment Analysis and Functional Annotation of Gene Lists (2021)." *Nucleic Acids Research* 50, no. W1: W216–W221.

Shields, E. J., L. Sheng, A. K. Weiner, B. A. Garcia, and R. Bonasio. 2018. "High-Quality Genome Assemblies Reveal Long Non-Coding RNAs Expressed in Ant Brains." *Cell Reports* 23, no. 10: 3078–3090. https://doi.org/10.1016/j.celrep.2018.05.014.

Team, R. C. 2023. "R: A Language and Environment for Statistical Computing." In *R Foundation for Statistical Computing*.

Wagner, G. P. 2014. "Homology, Genes, and Evolutionary Innovation." In *Homology, Genes, and Evolutionary Innovation*. Princeton University Press.

Ward, P. S., B. L. Fisher, J. J. Wernegreen, and B. B. Blaimer. 2025. "Evolutionary History, Novel Lineages and Symbiont Coevolution in the Ant Tribe Camponotini (Hymenoptera: Formicidae)." *Systematic Entomology* 50, no. 3: 646–676.

West-Eberhard, M. J. 2005. "Developmental Plasticity and the Origin of Species Differences." Supplement, *Proceedings of the National Academy of Sciences* 102, no. suppl_1: 6543–6549.

Wray, G. A. 2007. "The Evolutionary Significance of Cis-Regulatory Mutations." *Nature Reviews Genetics* 8, no. 3: 206–216.

Zhang, J. 2003. "Evolution by Gene Duplication: An Update." *Trends in Ecology and Evolution* 18, no. 6: 292–298.

Supporting Information

Additional supporting information can be found online in the Supporting Information section.
Figure S1: Principal component analysis (PCA) of transcriptomic samples. **Figure S2:** Graph representing the differences in bacterial transcriptome between the bacteriocytes and germline capsule. **Figure S3:** Phylogenetic relationship between ants of the tribe Camponotini. **Table S1:** The number of raw reads and cleaned reads from three replicates each of tissues and stages. **Table S2:** Output from GO terms and KEGG using DAVID platform for bacteriocytes versus germline capsule. **Table S3:** Output from GO terms and KEGG using DAVID comparing stage 5 versus bacteriocytes.